

# Titanium Water Heat Pipe Radiators for Space Fission System Thermal Management

Kuan-Lin Lee<sup>1</sup>, Calin Tarau<sup>2</sup> and William G. Anderson<sup>1\*</sup>

<sup>1</sup>Advanced Cooling Technologies, Inc., Lancaster, PA 17601, United State

## Abstract

For future space transportation and surface power applications, NASA Glenn Research Center (GRC) is currently investigating a small fission system (Kilopower system), which has operable range of 1 to 10kW<sub>e</sub>. The Kilopower system uses alkali metal heat pipes to transport heat from a nuclear reactor to the Stirling convertors to produce electricity and titanium water heat pipes to remove the waste heat from the convertors to the radiators. In a Small Business Innovation Research (SBIR) program, Advanced Cooling Technologies, Inc. (ACT) developed the titanium/water heat pipes for Kilopower waste heat rejection. These heat pipes are featured with bi-porous screen in the evaporator, and a screen-groove hybrid wick for the rest of the pipe, that allow the Kilopower system to survive and function under following four conditions: (1) space operation with zero gravity (2) ground testing with slight adverse gravity orientation (3) surface operation with gravity-aided orientation (4) and launch, with the against-gravity orientation and below freezing temperature. This paper presents the development of the titanium water heat pipes with radiator for Kilopower waste heat rejection, including the hardware design, heat pipe radiator assembly and thermal performance experimental validation.

*Keywords:* Bi-porous screen; Screen-groove hybrid wick; Titanium water heat pipe; Kilopower system

## 1. INTRODUCTION

For future space transportation and surface power applications, NASA Glenn Research Center (GRC) is leading the efforts to develop a small-scale nuclear fission power system (i.e. Kilopower system). This system is designed to provide 1 to 10 kW of electricity through Stirling conversion [1]. The conceptual design and the thermal management architecture of the Kilopower system can be seen in Fig. 1. Thermal energy of the nuclear reactor core is transferred to the Stirling convertor's hot end through a series of sodium heat pipes. After the energy conversion, the waste heat from the convertor's cold end is transferred to the radiator panels through multiple titanium water heat pipes and ultimately rejected into the space environment. Sponsored by a Small Business Innovation Research (SBIR) funding, Advanced Cooling Technologies, Inc (ACT) developed the titanium water heat pipes attached with radiator panel for Kilopower waste heat rejection [2] [3]. Each heat pipe needs to carry at least 125 Watts of waste heat during nominal operation and to carry 250 Watts at marginal conditions. The operating temperature of the Stirling convertor cold end should be maintained at 400K (~125°C). In addition, these titanium water heat pipes need to survive and function under the following operating conditions:

1. Space operation with zero-gravity.
2. Ground testing condition with a slight adverse gravity elevation (i.e. the evaporator is slightly higher than the condenser) to simulate microgravity operation.

3. Planetary surface operation with gravity-aided orientation, which is the simplest scenario.
4. Startup after being exposed to the launch condition. In such scenarios, heat pipes are orientated in an extreme against gravity and the sink temperature is lower than the freezing point of water.

This paper presents the development of titanium water heat pipes with radiator for Kilopower system waste heat rejection, including the hardware design, prototype development, deliverable heat pipes assembly and thermal performance experimental validation in a relevant environment.

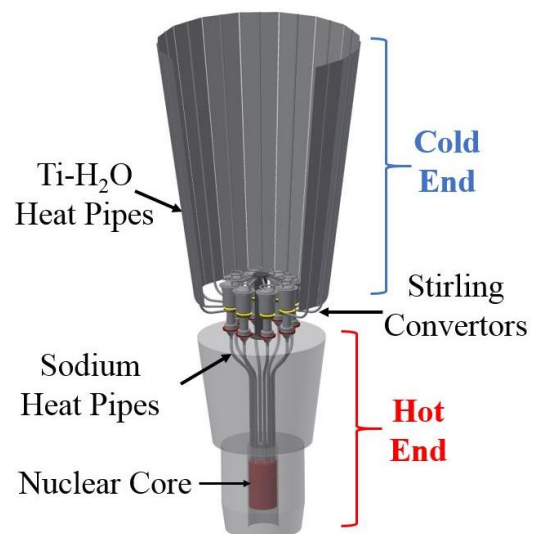


Fig. 1 Kilopower system conceptual design and the thermal management system [1]

## 2. HEAT PIPE DESIGN

To fulfill the design requirements stated above, the titanium water heat pipe has the unique bi-porous screen structure in the evaporator and the screen-groove hybrid wick structure at the adiabatic and the condenser sections.

### 2.1 Bi-porous screen evaporator

Two evaporator configurations were designed to accommodate different interfacing surfaces with the Stirling convertor. The direct interface evaporator is shown in Fig. 2(a), which directly clamps to the cylindrical portion of the Stirling convertor. The waste heat generated from the Stirling convertor transfers into the C-shape evaporator through its curved inner annular surface. The second evaporator (Fig. 2(b)) interfaces with the Stirling convertor via a Cold Side Adapter Flange (CSAF). In this interfacing mode, the waste heat from the Stirling convertor conducts through the CSAF and enters the evaporator from its flat bottom surface. Two types of titanium screen with different pore sizes (i.e. bi-porous screen) were inserted into the evaporator.

1. Fine screen meshes attached adjacent to the heating surfaces (i.e. inner annular and flat bottom) provide sufficient capillary action to pull the liquid working fluid from the grooved section to the heating surfaces.
2. Layers of coarse screen mesh occupying the remaining interior volume of the evaporator interior volume provide a storage volume to hold the entire liquid inventory of the grooved section during the launch condition. ACT named it the “accumulator”.

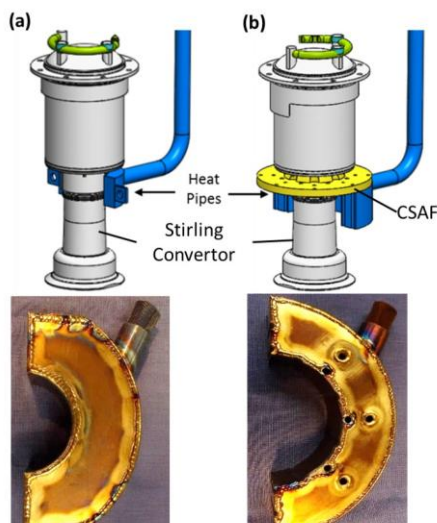


Fig. 2. Two evaporator configurations (a) Direct Interface evaporator (b) CSAF evaporator

To minimize liquid flow paths and the pressure drop across the accumulator, a section of grooved pipes extends into the evaporator and directly attaching to the primary fine screen. The working fluid flow paths and the arrangement of bi-porous screen inside an evaporator are shown in Fig. 3. During the launch period, the liquid inventory of grooves will temporary stores within the accumulator to prevent the damages of pipes and grooves while the liquid is being frozen. While startup, the liquid originally hold within the accumulator will be capillary driven by the primary screen and vaporized then re-distributed to the grooved section. The primary screen (i.e. fine screen) will be always saturated with the working fluid.

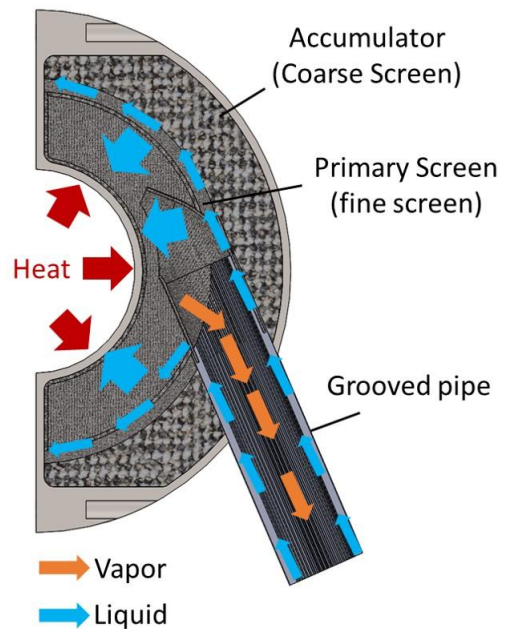


Fig. 3 section view of a direct interface evaporator

### 2.2 Grooved section optimization

The rest portion of the heat pipe (i.e. the adiabatic section and the condenser) has an axial grooves structure for liquid return during space operation. The geometry of grooves was designed based on a one-dimensional mathematical model, which was similar to Do's model [4]. The momentum equations of liquid phase and vapor phase (eqn. 1 and 2) were first solved with a given groove geometry and heat input. The variation of meniscus radius along grooves can then be determined by solving the Young-Laplace equation (eqn. 3). The relationship between the meniscus radius and the hydraulic parameters (e.g. diameter, liquid flow area and shear surface) within the grooves were determined by the

groove geometry. The iteration process was performed by the MathCAD to determine the maximum power capability.

$$\frac{dP_l}{dz} = \frac{-2(fRe)\mu_l Q}{D_{hl}^2 A \rho_l h_{fg}} S_{eff} - g \rho_l \sin \theta \quad (1)$$

$$\frac{dP_v}{dz} = f_v \frac{\rho_v v^2}{2D_{hv}} + g \rho_v \sin \theta \quad (2)$$

$$\frac{dr}{dz} = -\frac{r^2}{\sigma} \left( \frac{dP_v}{dz} - \frac{dP_l}{dz} \right) \quad (3)$$

An extensive trade study was performed to identify the optimum groove geometry that has the highest heat transport capability with lower structural mass and thermal resistance. Specifications of the finalized groove profile are summarized in Table 1 and the groove profile manufactured by electrical discharge machining (EDM) is shown in Fig. 4. For performance validation, ACT fabricated a 120 cm long groove heat pipe and tested its heat transport capability in various orientations and working temperature. The test results show a great match with the model prediction [3].

Table 1. Specifications of the grooved section

Pipe OD	1.59 cm
Adiabatic length	15.24 cm
Condenser length	100.0 m
Groove number	48
Groove depth	0.1 cm
Groove shape	Trapezoidal
Min. wall thickness	0.05 cm

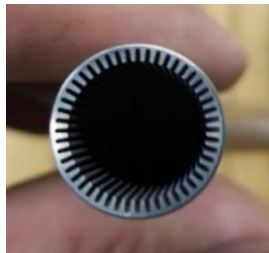


Fig. 4 EDM grooves

### 3. HEAT PIPE ASSEMBLY

A groove section needs to turn at  $\sim 82^\circ$  to avoid interference with the Stirling convertors. The grooved pipe was bent with salt particles or ice filled inside to prevent the collapse of pipe wall and the damage of grooves. After bending, multiple grooved

pipes sections were joined together through electron beam welding. The full-length ( $\sim 1$  m) grooved pipe was then coupled with the bi-porous screened evaporator through the screen-groove hybrid joint. Fig. 5 shows the titanium heat pipe before charging. The heat pipe was then charged with DI water, and a small amount of argon (NCG) to facilitate the startup process.

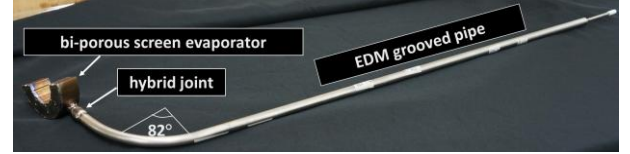


Fig. 5 Titanium water heat pipe with bi-porous screen evaporator and hybrid wick for the rest of the pipe.

## 4. EXPERIMENTAL VALIDATION

Three titanium water heat pipe prototypes were fabricated and tested. This section will present the experimental investigation of the last prototype (3<sup>rd</sup> prototype), which has a CSAF evaporator with bi-porous screen structure and axial grooves in the adiabatic and condenser sections.

### 4.1 Test setup

The experimental setup to validate the performance of the prototypes is shown in Fig. 6. Heat was applied to the evaporator by a CSAF mock heater. Cooling was provided by several chiller blocks with LN passing through. Chiller blocks were mounted on the top of the condenser section of the heat pipe. Temperature distribution along the heat pipe was measured by multiple T-type thermocouple probes welded to the surface of CSAF evaporator and along the adiabatic and condenser sections. To estimate pipe performance in microgravity, the heat pipe was orientated in such a way that the level of evaporator was slightly ( $\sim 0.25$  cm) above the condenser. Heat pipe working temperature was maintained through LN active cooling. The system was well-insulated to minimize heat leaks. As mentioned, NCG (argon) was charged to facilitate heat pipe startup.

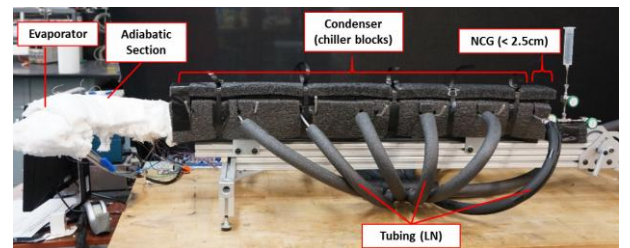


Fig. 6 Experimental system for titanium water heat pipe

## 4.2 Heat transfer performance

Test results of the prototype heat pipe at working temperature of 100°C is shown in

Fig. 7. ACT first started up the pipe through orienting the pipe in the gravity-aided inclination and applying a high power at 500W. Once the pipe started operating (t = 1800 second), it was placed in the slightly adverse gravity orientation (~ 0.25 cm adverse inclination) and the heat input was turned down to 125W. Heat pipe reached a steady-state at 3500 second. A uniform temperature distribution can be seen from the instantaneous temperature profile (Fig. 8). The temperature difference between evaporator and condenser was 2.8°C. Subsequently at t=6200 second, power was turned up to 200W and then to 250W. The heat pipe reached another steady state at t=9000 second. The corresponding temperature profile is shown in Fig. 9. At Q=250W, temperature difference increased to 4.9°C.

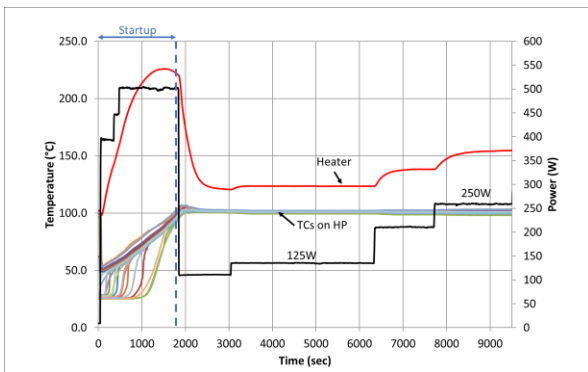


Fig. 7 Temperature profile variation with time (working temperature of 100°C, evaporator was elevated 0.25 cm higher than the condenser).

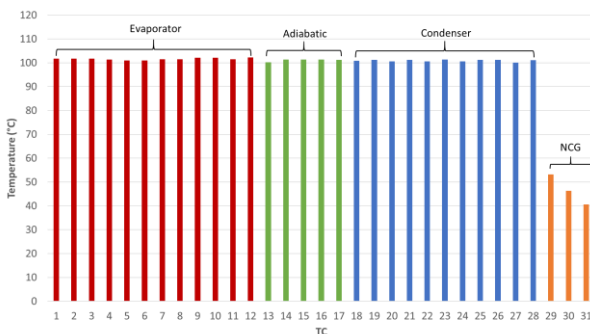


Fig. 8. Instantaneous temperature distribution along the heat pipe at t= 5500 sec (Q=125W)

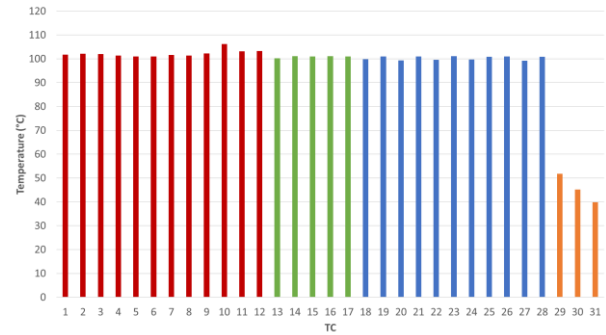


Fig. 9. Instantaneous temperature distributions along the heat pipe at t= 9100 sec (Q=250 W)

Fig. 10 below shows the thermal resistance of the prototype heat pipe at working temperature of 125°C with different heat inputs (50W - 450W) and in various orientations (horizontal, 0.25cm adverse gravity, 0.51cm adverse gravity and gravity-aided). As the figure indicates, the heat pipe prototype is capable of carrying 450W of heat at 0.25 cm adverse gravity elevation. The average thermal resistance of the prototype heat pipe shown in the plot is at 0.01 °C/W.

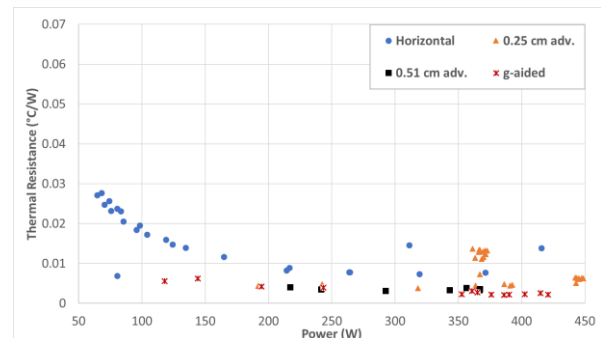


Fig. 10. Thermal resistance dependence on different adverse gravity elevations (working temperature at 125°C)

## 4.3 Freeze/thaw startup performance

An extensive freeze-thaw testing was performed. As Fig. 11 shows, the prototypic heat pipe in a slight against gravity orientation was first operating in the steady-state at 125°C working temperature with 250W heat input (state 1). At 1000 second, heat input was removed and the entire system (including the mock heater) was cooled to -50°C by LN. At 2000 second, heat was re-applied to startup the pipe. Heat input was steadily increased from 125W to 250W. As the figure shows, a smooth freeze/thaw recovery curve was obtained. As the working temperature reached 125°C at t=10500 second, the LN active cooling

was ON again to maintain the working temperature. The heat pipe operated at the same steady state parameters as in the beginning of the test (state 1). Temperature distribution along the pipe at both the frozen state ( $t=1900s$ ) and the steady-state ( $t=11000s$ ) are shown in Fig. 12. This test demonstrates that the special bi-porous screen evaporator design and NCG charged enable the heat pipe to survive and to recover from a deeply frozen condition.

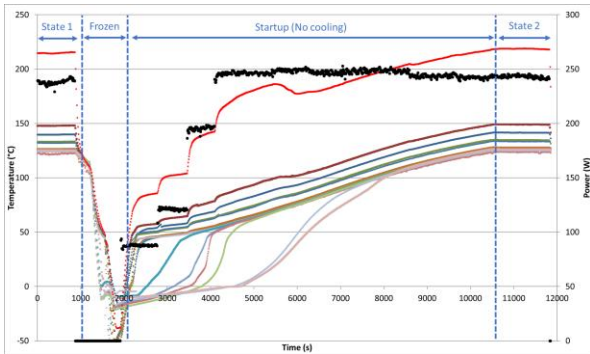


Fig. 11. Freeze/thaw startup performance of the titanium water heat pipe

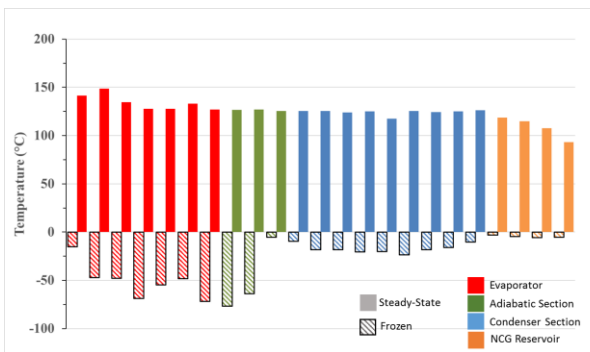


Fig. 12 Corresponding instantaneous temperature distributions along the heat pipe at frozen state ( $t= 1900$  sec) and the steady-state ( $t=11000$  sec)

## 5. DELIVERABLE HEAT PIPES DEVELOPMENT

### 5.1 List of deliverables

Following the similar fabrication procedure as the 3<sup>rd</sup> prototype, ACT further fabricated 7 titanium heat pipes (6 of them has radiator attached) which will be tested on a Kilopower technology demonstration system in NASA Glenn Research Center (GRC). As summarized in Table 2, these deliverable heat pipes are 6 full-length titanium water heat pipes with radiator attached and 1 half-length heat pipe without radiator for shock and vibration testing. HP-A and HP-B are in pair, which will interface with a top Stirling convertor

via CSAF. As Fig. 13 depicts, the location of top Stirling convertor is closer to the radiator side of the Kilopower system, therefore the heat pipes require shorter grooved sections. HP-C and HP-D have direct interface evaporators, which will directly clamp on the cylindrical portion of the top Stirling convertor. HP-E and HP-F with longer grooved sections will interface with the bottom Stirling convertor via CSAF. HP-G is a half-length heat pipe without radiator attached, only for shock and vibration testing.

Table 2. List of deliverable heat pipes

HP No.	Evaporator	Grooved Pipe Length (cm)	Radiator
A	CSAF Interface	113.03	O
B	CSAF Interface	113.03	O
C	Direct Interface	113.03	O
D	Direct Interface	113.03	O
E	CSAF Interface	130.18	O
F	CSAF Interface	130.18	O
G	Direct Interface	60.96	X

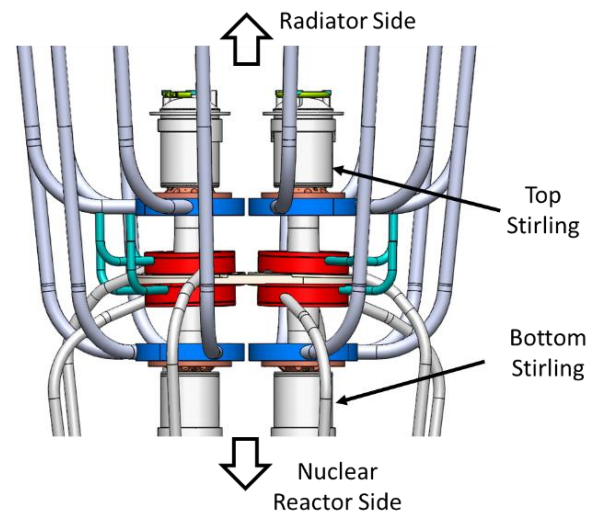


Fig. 13. Relative locations of titanium water heat pipe (blue) and the Stirling convertors.

### 5.2 Radiator attachment

Thin aluminum panels (0.03 cm) were integrated to the condenser section of the titanium heat pipe as the radiator panels. The total area of the radiator panel was designed to be 15.24 cm by 91.44 cm. To

reduce the thermal expansion mismatch issue while bonding two dissimilar (Ti and Al), a novel active solder called S-bond was employed [5]. The bonding integrity and the interfacial thermal resistance of S-bond had been validated by ACT in previous research [3]. After S-bonding, the surfaces of radiator were painted with Aeroglaze A276 to have a higher radiation emissivity at 0.86. The deliverable heat pipes with aluminum radiator panel are shown in Fig. 14 below. After charging with water and argon, the full-length heat pipes were ready for testing in a thermal vacuum chamber.

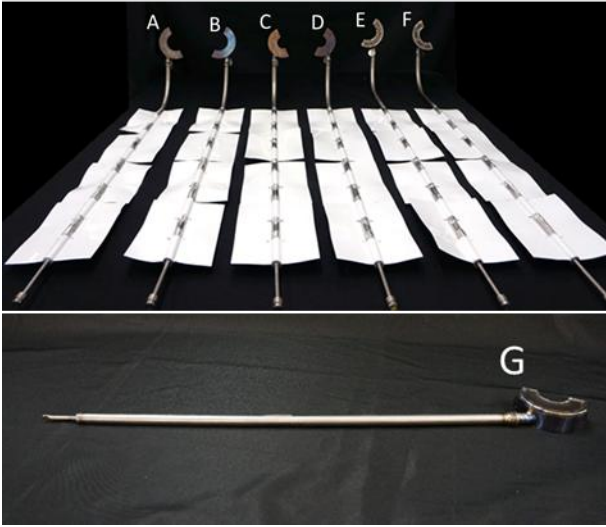


Fig. 14 Titanium water heat pipes for Kilopower system cooling (top: six full-length heat pipes with S-bonded radiator; bottom: half-length heat pipe for shock and vibration testing)

### 5.3 Thermal vacuum chamber (TVC) test

To simulate a space operation, the deliverable heat pipes with radiator were tested in a thermal vacuum chamber in a slight against gravity orientation ( $\sim 0.25$  cm elevation). The test setup is shown in

Fig. 15. Heat was provided by CSAF or direct interface mock heaters and the radiation cooling was provided by two aluminum plates with LN pipelines attached (cold walls). The heat pipe radiator was sandwiched between two cold walls without physical contacts. In this set of experiment, instead of keeping the working temperature at a constant of  $125^{\circ}\text{C}$ , ACT maintained the sink temperature (cold wall) at  $300\text{K}$ . TC instrumentation can be seen from the TC map (Fig. 16). Note that all TCs along the condenser section were attached to the radiator surface rather than the pipe surface. At the end of radiator, a portion of  $3.81\text{cm}$  away from the fill tube was considered to be the NCG reservoir, being covered by TCs 18, 20 and 21. Additional temperature probe (TC 19) was attached to the tips of the radiator to study the fin efficient.

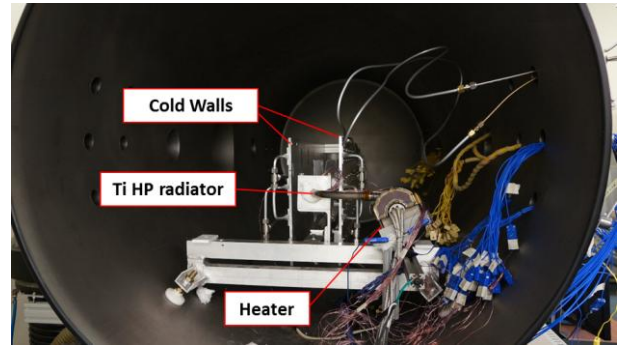


Fig. 15 Heat pipe radiator thermal performance test setup

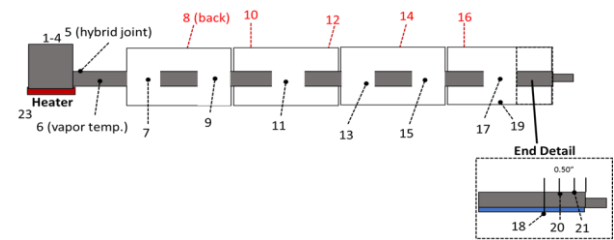


Fig. 16. TC map of heat pipe radiator

The test procedure is as follows:

1. Evacuate TVC until the internal pressure is less than 1 torr.
2. Apply heat to the evaporator incrementally from  $125\text{W}$  to  $250\text{W}$
3. Maintain the average cold wall temperature at  $300\text{K}$  through active cooling.

### 5.4 TVC test results

Fig. 17 shows the thermal performance of HP-F, which is considered to be the most representative design because it has the longest grooved section and the most complex evaporator geometry (CSAF type), making the liquid return more challenging than others. The heat pipe radiator started up and reached the steady-state immediately as the heat was applied at  $t=700$  second. Heat inputs was then gradually increased to  $250\text{W}$  with the sink temperature maintained at  $300\text{K}$ . No dry-out were observed, proving that the heat pipe radiator is able to reject  $250\text{W}$  of heat in a space-like environment. The temperature profile at two steady-states are shown in Fig. 18 and Fig. 19. When  $Q=125\text{W}$ , vapor temperature (i.e. adiabatic section) is  $120^{\circ}\text{C}$ , the base temperature of the radiator (condenser) is  $119.8^{\circ}\text{C}$  and the fin tip temperature (purple line) is  $95^{\circ}\text{C}$ . The fin efficiency and the overall thermal

resistance are 0.583 and 0.019 °C/W. When  $Q=250\text{W}$ , vapor temperature increases to  $180^{\circ}\text{C}$ , the radiator base temperature is  $179.4^{\circ}\text{C}$  and the fin tip temperature is  $135.4^{\circ}\text{C}$ . The corresponding fin efficiency and the overall thermal resistance are 0.54 and  $0.023^{\circ}\text{C/W}$ . Note that the overall thermal resistance mentioned here is the addition of the resistance of heat pipe, the contact resistance of S-bond joint and the resistance across the thin aluminum panel.

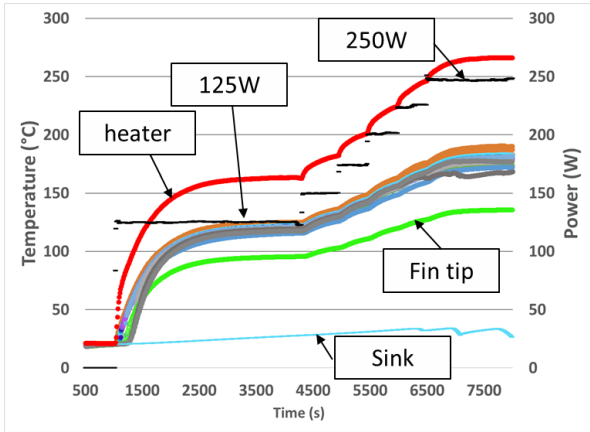


Fig. 17 Thermal performance test results of heat pipe radiator “F”

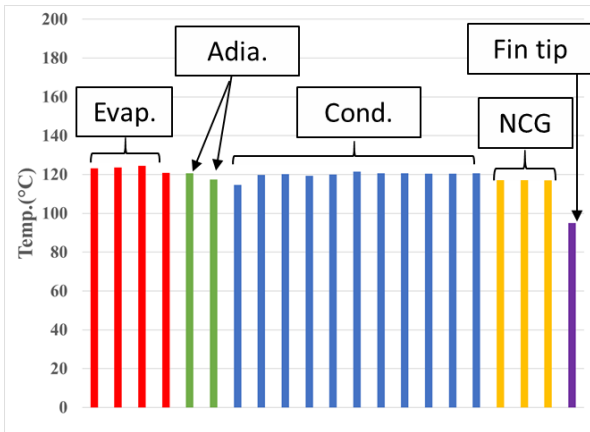


Fig. 18 Instantaneous temperature distributions along the heat pipe at  $t= 3740\text{ sec}$  ( $Q=125\text{W}$ )

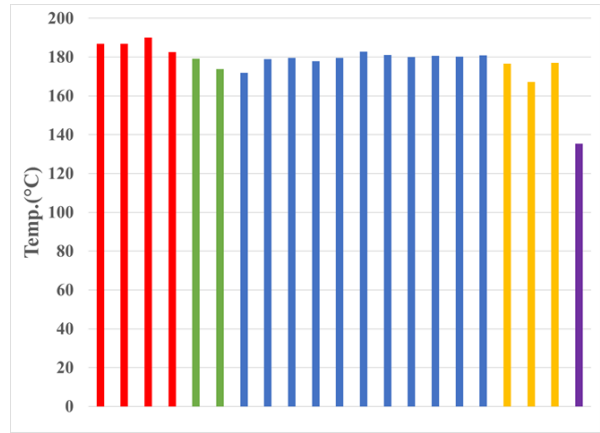


Fig. 19 Instantaneous temperature distributions along the heat pipe at  $t= 7676\text{ sec}$  ( $Q=250\text{W}$ )

Other heat pipe radiators (from HP-A to HP-E) were tested through the identical procedure. All heat pipes were successfully rejected the nominal power in a space-like condition. The corresponding thermal resistance and the total weight of each heat pipe radiator are summarized in Table 3. It can be seen that the heaviest deliverable is at 0.73 kg.

Table 3. Summary of HP radiator performance

HP radiator	Thermal Resistance ( $^{\circ}\text{C/W}$ )	Total weight (kg)
A	0.075	0.695
B	0.036	0.685
C	0.057	0.665
D	0.048	0.655
E	0.019	0.730
F	0.036	0.715

The half-length heat pipe was qualified through IR imaging as Fig. 20 shows. A uniform temperature distribution can be observed.

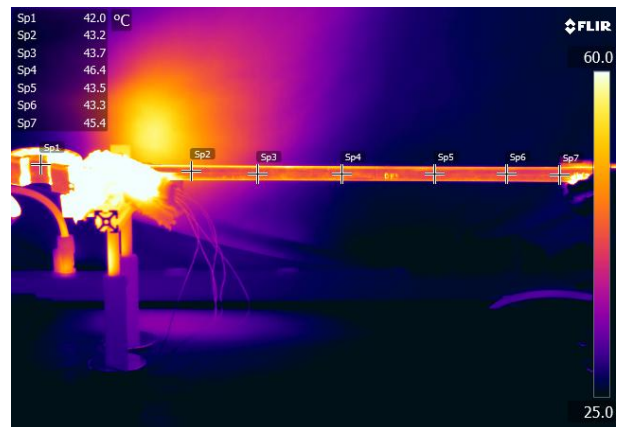


Fig. 20 IR image of HP-G in a horizontal orientation

## 6. CONCLUSIONS

ACT developed a series of titanium water heat pipe with aluminum radiator attached to reject the waste heat of a small-scale space nuclear fission power system (i.e. Kilopower system). These titanium heat pipe has bi-porous screen structure in the evaporator and axial groove structure in the adiabatic and condenser sections. The prototypic heat pipe was fabricated and tested, which shown good heat transfer capability and isothermality in a slight against gravity orientation. Its freeze/thaw tolerance feature was also demonstrated. Afterward, 7 titanium water heat pipes, which have different evaporator configurations (CSAF and direct interface) and various grooved pipe lengths were fabricated and tested. Six of the titanium heat pipes were integrated with aluminum facesheets through S-bonding then tested in a thermal vacuum chamber. All six heat pipe radiators successfully carried 125W of waste heat at the working temperature of 400K and rejected to the vacuum environment through radiation. The deliverables (7 titanium water heat pipes) have been sent to NASA GRC for further performance validation.

## ACKNOWLEDGEMENTS

This research was sponsored by NASA Glenn Research Center under Contract NNX15CC06C. ACT would like to thank Maxwell Briggs, Marc Gibson, Jim Sanzi, and Lee Mason for their support and helpful discussions during the program. In addition, special thanks are addressed to Philip Texter, Larry Waltman and Tim Wagner who were the technicians on the program at ACT.

## NOMENCLATURE

$A$	: liquid flow area
$D_h$	: hydraulic diameter
$fRe$	: Poiseuille number for a trapezoidal groove
$f_v$	: Vapor friction factor in a circular pipe
$g$	: gravity ( $9.8 \text{ m/s}^2$ )
$h_{fg}$	: latent heat of vaporization
$P$	: pressure
$Q$	: heat input
$r$	: meniscus radius
$S_{eff}$	: shear area between liquid and vapor flow
$v$	: speed of vapor flow
$z$	: axial direction
$\theta$	: Inclination angle (rad)
$\rho$	: density
$\mu$	: viscosity (Pa-s)

## REFERENCES

- [1] M. A. Gibson, S. R. Oleson, D. I. Poston and P. McClure, "NASA's Kilopower Reactor Development and the Path to Higher Power Missions," in *IEEE Aerospace Conference*, Big Sky, MT, 2017.
- [2] R. Hay and W. G. Anderson, "Water-Titanium Heat Pipes for Spacecraft Fission Power," in *International Energy Conversion Engineering Conference (IECEC-AIAA)*, Orlando, FL, 2015.
- [3] D. Beard, W. G. Anderson, M. Ababneh, B. Schwartz and K.-L. Lee, "High Temperature Water Heat Pipes for Kilopower System," in *International Energy Conversion Engineering Conference*, Atlanta, GA, 2017.
- [4] K. H. Do, S. J. Kim and S. V. Garimella, "A mathematical model for analyzing the thermal characteristics of a flat micro heat pipe with a groove wick," *International Journal of Heat and Mass Transfer*, vol. 51, pp. 4637-4650, 2008.
- [5] S-bond Technologies, "S-bond Technologies," [Online]. Available: <http://www.s-bond.com/>.

---

\*Corresponding author: bill.anderson@1-act.com, Phone: 717-205-0602